Tree Physiology Advance Access published January 6, 2012

Tree Physiology 00, 1–12
doi:10.1093/treephys/tpr133

Research paper

Increased resin flow in mature pine trees growing under elevated CO_2 and moderate soil fertility

K.A. Novick[1,2,5], G.G. Katul[1], H.R. McCarthy[3] and R. Oren[1,4]

[1]Nicholas School of the Environment and Pratt School of Engineering, Duke University, Box 90328, Durham, NC 27708, USA; [2]Present address: USDA Forest Service, Southern Research Station, Coweeta Hydrologic Laboratory, Otto, NC 28763, USA; [3]Department of Botany and Microbiology, University of Oklahoma, Norman, OK 73019, USA; [4]Department of Forest Ecology & Management, Swedish University of Agricultural Sciences (SLU), SE-901 83, Umeå, Sweden; [5]Corresponding author: Coweeta Hydrologic Laboratory, 3160 Coweeta Lab Road, Otto, NC 28763, USA (kimberlynovick@fs.fed.us)

Received April 12, 2011; accepted November 19, 2011; handling Editor Yann Nouvellon

Warmer climates induced by elevated atmospheric CO_2 (eCO_2) are expected to increase damaging bark beetle activity in pine forests, yet the effect of eCO_2 on resin production—the tree's primary defense against beetle attack—remains largely unknown. Following growth-differentiation balance theory, if extra carbohydrates produced under eCO_2 are not consumed by respiration or growth, resin production could increase. Here, the effect of eCO_2 on resin production of mature pines is assessed. As predicted, eCO_2 enhanced resin flow by an average of 140% ($P = 0.03$) in canopy dominants growing in low-nitrogen soils, but did not affect resin flow in faster-growing fertilized canopy dominants or in carbohydrate-limited suppressed individuals. Thus, pine trees may become increasingly protected from bark beetle attacks in an eCO_2 climate, except where they are fertilized or are allowed to become overcrowded.

Keywords: bark beetles, carbon allocation, Free Air CO_2 Enrichment, *Pinus taeda*, resin flow, resistance.

Introduction

Bark beetles (Curculionidae: Scolytinae) and their fungal associates are among the most ecologically altering and economically damaging natural disturbance agents in coniferous forests (Price et al. 1998, Kurz et al. 2008, Raffa et al. 2008). Several studies predict increases in beetle activity in warmer climates or cite higher air temperatures as a co-factor in recent beetle outbreaks (Logan et al. 2003, Gan 2004, Berg et al. 2006, Kurz et al. 2008). However, future forest-beetle dynamics also depend on the response of the host's defense mechanisms to climate and atmospheric changes, and these have not yet been determined (Negron et al. 2008). In particular, the effect of elevated atmospheric CO_2 on resin production in mature pine trees—a primary defense against bark beetle attack—has not been quantified.

Resin production is largely, though not exclusively, a mechanical defense strategy. Resin physically ejects or entombs attacking beetles and, when volatile components of resin have evaporated, seals wounds in the bark (Ruel et al. 1998, Wilkens et al. 1998). Resin flow may be either constitutive or induced, where the former represents the flow of a standing pool of resin formed in the tree prior to attack, and the latter represents the de novo synthesis of resin following mass wounding events associated with a high density of beetle attacks (Lombardero et al. 2000). Results from previous studies suggest that both constitutive and induced resin flow play an important role in defending pine trees from attacking beetles (Reeve et al. 1995, Lorio et al. 1995, Strom et al. 2002, Wallin et al. 2008). This study is focused on the effects of atmospheric CO_2 concentration, as well as soil nutrient availability, canopy position and time of year, on constitutive resin flow in mature loblolly pine trees, noting that the mass wounding treatments necessary to produce induced resin flow were not permissible in the Free Air CO_2 Enrichment (FACE) setting, where this study took place. Our hypotheses and the interpretation of our results are framed by the following theoretical considerations.

Early work on the resistance of pines to bark beetle attacks suggested that resin production was a reflection of tree vigor, such that a scarcity of photosynthates from environmental- or competition-caused stress decreases both tree growth and resistance (Waring and Pitman 1985). Other studies demonstrated that resin flow could be increased even as growth or vigor decreased through manipulations of soil nutrients, moisture and stand density, provided that reductions in photosynthesis were less than reductions in growth (Lorio 1986, Lorio et al. 1995, McDowell et al. 2007, Knebel et al. 2008). The notion that growth and secondary processes (such as resin production) are competing sinks for assimilated carbon is a central component of the 'growth-differentiation balance' (GDB) hypothesis for plant defense, first applied to pines by Lorio (1986) and later formalized by Herms and Mattson (1992).

Foremost, the GDB hypothesis predicts that, when herbivory levels are low, assimilated photosynthates are preferentially allocated to maintenance and growth processes over secondary processes such as resin synthesis, and thus constitutive resin production will be directly correlated to the balance between two quantities: (i) the rate of production of available carbohydrates (A'), here defined as gross primary production (GPP) less maintenance respiration (i.e., $A' = \mathrm{GPP} - R_M$), and (ii) the rate at which available carbohydrates are used in primary growth processes, or net primary production (NPP). When A' is limited by some factor (F), an increase in F will tend to increase A' more than NPP (Phase I of Figure 1). Here, F represents any variable that is potentially limiting to A' and that changes in time and/or space, including soil nutrient and moisture availability, light availability and temperature. Thus, in Phase I, $\partial(A' - \mathrm{NPP})/\partial F > 0$, and the balance $A' - \mathrm{NPP}$ widens with increasing F (Figure 1a and b). As a result, in Phase I, positive relationships among A', NPP, $A' - \mathrm{NPP}$ and resin production are expected.

When F is no longer limiting to A' (Phase II), A' reaches saturation with increasing F (Figure 1a, $\partial A'/\partial F \approx 0$) while NPP continues to increase (Palmroth et al. 2006) so that $\partial(A' - NPP)/\partial F < 0$. Thus, in Phase II, the GDB hypothesis suggests an inverse relationship between NPP and resin production due to competition for limited carbohydrates (Herms and Mattson 1992). Consequently, the sign of $\partial(A' - \mathrm{NPP})/\partial F$ determines whether resin production increases or decreases with changes in F. While the hypothesis is generally presented and interpreted over a spatial or temporal gradient of a single resource, the framework may be generalized such that $F = (F_1, F_2, \ldots)$ represents a vector of factors that vary in time and space. In this case, resin production is correlated with the sign of the aggregated sum of $\mathrm{d}(A' - \mathrm{NPP})$, given as

$$\mathrm{d}(A' - \mathrm{NPP}) = \frac{\partial(A' - \mathrm{NPP})}{\partial F_1}\mathrm{d}F_1 + \frac{\partial(A' - \mathrm{NPP})}{\partial F_2}\mathrm{d}F_2 + \ldots. \quad (1)$$

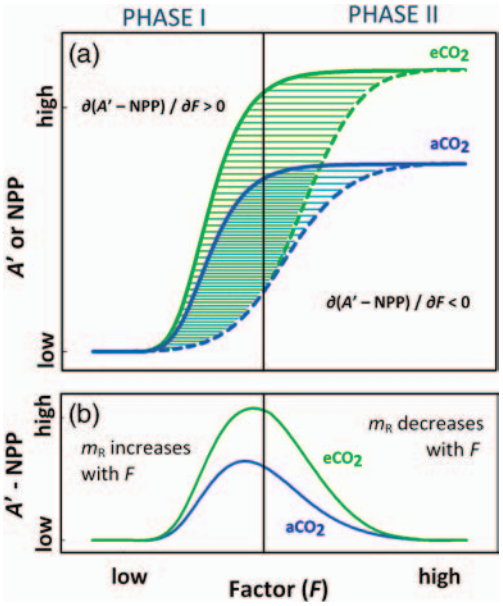

Figure 1. The growth-differentiation balance hypothesis. (a) Conceptual change in available photosynthates (A', solid lines) and growth processes (NPP, dashed lines) with a factor F, where F may be any potentially limiting resource. Shaded areas show the pool of excess carbohydrates available for secondary processes like resin synthesis ($A' - \mathrm{NPP}$), which is also shown separately in (b). In Phase I, A' increases faster than NPP (i.e., $\partial A'/\partial F > \partial \mathrm{NPP}/\partial F$) such that $A' - \mathrm{NPP}$ also increases with F. In Phase II, A' approaches its maximum so that $\partial A'/\partial F < \partial \mathrm{NPP}/\partial F$ and $A' - \mathrm{NPP}$ decreases with F. Thus, the sign of $\partial(A' - \mathrm{NPP})/\partial F$ dictates the sign of the change in resin flow (m_R) with F. The trends for ambient and elevated CO_2 show that the $A' - \mathrm{NPP}$ balance can be larger under elevated CO_2 for mid-range F. The figure is adapted from Figure 1 in Herms and Mattson (1992).

Based on this framework, it is possible to predict how spatial and temporal gradients in factors known to impact A' may affect resin production. Specifically, elevated CO_2 should increase resin production in low- to mid-range fertility by increasing A' while NPP is limited by nutrient availability (Figure 1). However, as soil fertility increases, growth restrictions are eased (Oren et al. 2001, Stamp 2004, Palmroth et al. 2006, McCarthy et al. 2007) and the eCO_2-induced enhancement of resin production is expected to decline. Resin production should be lower in suppressed as compared with dominant individuals as A' is limited for the former by low light availability in the sub-canopy. Over the course of a growing season, a period exists in which light intensity, day length, temperature and leaf area index are sufficiently high and stable, shifting forest canopies from Phase I (when A' is limited by these factors) to Phase II (when A' is relatively high and stationary). During that stable A' period, temporal variation in factors such as soil moisture introduces variation in NPP. Thus, as the shift occurs, the sign of $\partial(A' - \mathrm{NPP})/\partial F$ will change, and the relationship between NPP and resin production should accordingly be positive in Phase I and negative in Phase II (see Figure 1).

In this study, components of *A′*, NPP and resin production are measured on a monthly basis in plots of mature, field-grown pine trees experiencing both ambient and elevated atmospheric CO_2 concentrations and a wide range of soil fertility. Results are interpreted within the context of these predictions from GDB theory (guided by Figure 1), and the trade-offs between growth and defense processes are discussed with consideration of forest management strategies in future climate conditions.

Methods

Setting

Components of *A′*, NPP and resin production were measured in the Duke FACE study (Hendrey et al. 1999), set in a 27-year-old *Pinus taeda* L. (loblolly pine) plantation in the Duke Forest, NC, USA. The pine plantation was established in 1983 following a clear cut and a burn. *Pinus taeda* L. (loblolly pine) seedlings were initially planted at a 2.0 m by 2.4 m spacing, and pine density was ~1100 trees hectare^{-1} in 1999 (Hendrey et al. 1999). Tree height approached 20 m at the time of this study. The stand has not been managed after planting and a diverse sub-canopy has developed consisting of *Liquidambar styraciflua* L. and nearly 40 other hardwood species.

The FACE facility comprises eight circular, 30 m diameter plots—four under ambient CO_2 concentrations (aCO_2) and four under elevated concentrations (eCO_2; ambient + 200 ppm). One ambient plot and one elevated plot comprise the FACE prototype complex, which has operated since 1994. The six remaining FACE plots have operated since 1996 as blocked replicates. Annual nitrogen (N) fertilization of half of each plot began several years after fumigation was initiated (Oren et al. 2001, Palmroth et al. 2005). This split-plot amendment created 16 subplots—four each of unfertilized and fertilized aCO_2 plots (AC and AF, respectively), and four each of unfertilized and fertilized eCO_2 plots (EC and EF). The prototype and replicated FACE plots are treated as one replicated experiment following initial analysis that failed to show a significant block effect on resin flow ($P = 0.62$ from a split-plot analysis of variance (ANOVA) with block as a random effect) and prior results that strongly reject the hypothesis that the prototype and replicated FACE complexes are not from the same study (McCarthy et al. 2007).

This study altered components of the $A' - \text{NPP}$ balance experimentally with eCO_2 and with fertilization, but also utilized natural resource gradients known to affect carbon assimilation and growth. Experimental plots cover a wide range of native N availability (from 2.6 to 5.0 g mineral N m^{-2}). Native N availability has been previously shown to be directly related to initial stand biomass (i.e., biomass before the onset of the FACE experiment), to stand-level NPP in both aCO_2 and eCO_2 (McCarthy et al. 2010), and to canopy leaf area (McCarthy et al. 2007). Furthermore, tree density in the FACE plots is sufficiently high to cause canopy class differentiation between suppressed, shaded individuals and dominant individuals provided with ample light. Hence, the Duke FACE facility provides a unique setting for evaluating GDB predictions of the effect of eCO_2, nutrient availability and canopy position on resin production.

Resin measurements

Resin mass flow (m_R) was measured monthly from March to October of 2009 in two canopy classes: dominant and suppressed trees. In each subplot, m_R was measured in three dominant trees and two suppressed trees with two subsamples per tree taken from opposite sides of the trunk. Following standard practice (Lombardero et al. 2000, Knebel et al. 2008), resin flow was measured by removing a 0.8 cm disk of bark to the phloem–xylem interface at breast height, and installing trays below the wound to direct the flow of resin into pre-weighed collection vials for a 24-h period. Vials were installed on all trees between 08:00 and 12:00 a.m. to minimize the effect of time-of-day variation on resin flow. Measurements were repeatedly conducted on the same set of trees, and care was taken to ensure that new wounds were laterally displaced at least 5 cm from previous wound sites. Using a lateral displacement distance of at least 5 cm is standard practice in constitutive resin flow studies and reflects the common assumption that the scarcity of radial resin duct connections limits the effect of previous resin flow measurements on subsequent sampling events (Ruel et al. 1998, Knebel et al. 2008). The resin flow measurements are normalized by the area of the wound and expressed in units of g cm^{-2} day^{-1}. It is important to note that while the resin flow measurements are referenced to the area of the wound (~0.50 cm^2), the longitudinal resin canal lengths are on the order of ~10 cm (Lapasha and Wheeler 1990). Thus, for a wound diameter of 0.8 cm, resin flows from an area of the phloem that is at least ~8 cm^2, and probably larger if any radial duct connections exist.

Assimilation and NPP

Gross ecosystem productivity (GEP) under ambient CO_2 (GEP_{aCO_2}) was estimated using eddy-covariance measurements of the net ecosystem exchange of CO_2 (NEE) and was used as a proxy for *A′*. Gross ecosystem productivity is defined as GPP less the amount of CO_2 that is internally recycled within the ecosystem, either by re-assimilation within the leaf of CO_2 produced by dark respiration, or by re-assimilation of respired CO_2 occurring within the canopy below the eddy-covariance instrumentation. Thus, GEP and GPP are analogous, but not identical (Goulden et al. 1997, Stoy et al. 2006). Measurements were subjected to quality control procedures to remove excessive sensor noise and data collected under very stable conditions. First, spikes in the data record were removed using the algorithm recommended for FLUXNET (Papale et al. 2006). Net

ecosystem exchange of CO_2 fluxes was then filtered to remove data collected during stable atmospheric conditions using a u* filtering method (Reichstein et al. 2005). Finally, fluxes were rejected if they exceeded a conservative window of −0.5 to 0.85 mg C m^{-2} s^{-1} in accordance with data quality control procedures previously employed at this site (Stoy et al. 2006). Note that a positive flux denotes assimilation by the ecosystem. Net ecosystem exchange of CO_2 was partitioned into GEP_{aCO_2} and ecosystem respiration using the non-rectangular hyperbola model described in Stoy et al. (2006).

The eddy-covariance estimates of GEP_{aCO_2} are stand-scale estimates, and no attempt was made to use these measurements to derive tree-level assimilation or to quantify the magnitude of stand-scale assimilation in eCO_2 plots. This time series was used only to identify the temporal pattern of assimilation. The dynamics of GEP are assumed to be similar under all treatments but vary in absolute magnitude with CO_2, and N and light availability. This assumption is supported by the results of earlier studies conducted at the Duke FACE facility, showing that monthly measurements of net leaf-level assimilation rate (A_{net}) are strongly correlated in aCO_2 and eCO_2 trees ($r = 0.93$, Figure 2a; Ellsworth 1999) and trees from unfertilized and fertilized sectors ($r = 0.86$, Figure 2b; Maier et al. 2008). Coupled with the additional similarity among treatments of the temporal dynamics of total leaf area (McCarthy et al. 2007), it is not surprising that Schäfer et al. (2003) found that the seasonal pattern of canopy-scale GPP estimated with the multi-layer, canopy conductance-constrained carbon assimilation model (4C-A) was similar under eCO_2 and aCO_2; furthermore, the pattern was consistent with eddy-covariance estimates of GEP. Thus, we conclude that the seasonal pattern of GEP_{aCO_2} was a reasonable proxy of A' of all treatments and both size classes, and can be used to partition the study period between periods of stable A' and periods of variable A'.

Net primary productivity of woody biomass (NPP_W), used as a proxy for NPP, was estimated on a monthly time step as the sum of the production of stems, branches and coarse roots. The stem and branch biomass values of individual trees were calculated allometrically using recently developed, site-specific relationships that are driven by both tree diameter and height (McCarthy et al. 2010). Monthly diameter increments were estimated by interpolating bi-weekly dendrometer measurements and determining the change in diameter from the beginning to the end of the month, noting that resin measurements were performed at the end of each month. Tree height increment measured on an annual basis was interpolated to monthly values using the same seasonal pattern of diameter growth. Plot-level coarse root biomass (>2 mm) was calculated as a function of aboveground biomass (Johnsen et al. 2004). Because NPP_W was estimated monthly, we accounted for the transition between earlywood and latewood, where latewood has twice the specific gravity of earlywood. The date of transition was estimated for each tree as the date at which the cumulative diameter increment, normalized by the total annual diameter increment, exceeds the treatment-specific earlywood fraction previously determined from analysis of growth rings.

Nitrogen availability

Nitrogen losses from the FACE study site have been shown to be negligible (Phillips et al. 2001, Finzi et al. 2006); thus, mineral N availability was estimated as the sum of N mineralization, N deposition, N fixation and N addition via fertilization. Annual N mineralization was measured over 3 separate years (1998, 2003 and 2005) using a buried-bag approach (Finzi et al. 2006, McCarthy et al. 2010). Nitrogen fixation rates were measured on five separate occasions between 2001 and 2003 by applying the acetylene reduction assay to soil cores and forest floor samples from each subplot (Hofmockel and Schlesinger 2007). Nitrogen deposition was estimated by Sparks et al. (2008) using a combination of eddy-covariance measurements of the flux of NO, local- and regional-scale

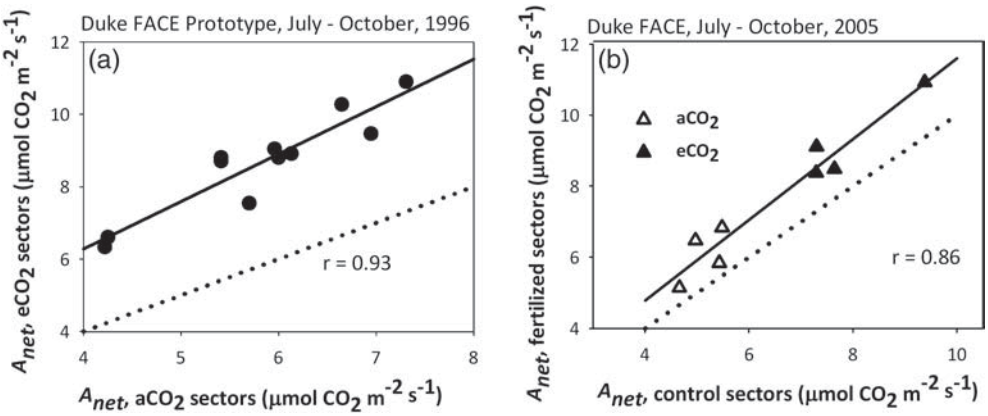

Figure 2. Temporal correlation of CO_2 assimilation rates (A_{net}) derived from leaf-level gas-exchange measurements. (a) Bi-weekly measurements performed in ambient CO_2 (aCO_2) and elevated CO_2 (eCO_2). Data are from Ellsworth (1999). (b) Monthly estimates of A_{net} from control and fertilized sectors of both CO_2 treatments. Data from Maier et al. (2008). Both datasets are from measurements made on current-year sunlit foliage. The dotted lines are 1:1 lines, shown for reference.

concentration measurements of other relevant N-containing species, and modeling techniques. The quantity of N added by fertilization is uniform across subplots (Oren et al. 2001), and mineral N availability in fertilized subplots was assumed to increase by ~5.5 g N m^{-2} over native N availability, consistent with previous studies (McCarthy et al. 2007).

Statistical analyses

Unless otherwise noted in the text, the significance of the difference in m_R between any two populations was evaluated using a two-tailed *T*-test assuming unknown means and equal variances. The significance of eCO_2, fertilization and time of year effects, and their interactions, on m_R was also evaluated separately for dominant and suppressed populations using a repeated-measures, split-plot ANOVA with CO_2 concentration as the main effect and fertilization treatment as the split effect.

Results

The study period and characteristics of the time series

The year 2009 was a relatively cool, wet year for the Duke FACE facility. Mean annual temperature was 14.4 °C, which is less than the long-term mean annual temperature (15.5 °C). Total annual precipitation at the Duke FACE facility in 2009 was 1231 mm, which is greater than the long-term mean of 1146 mm. Mean monthly temperature during the study period was highest in August (Figure 3a).

Canopy assimilation (i.e., GEP_{aCO_2}) was relatively low in March, April, September and October in response to reduced leaf area and unfavorable climatic conditions. Gross ecosystem productivity under ambient CO_2 was relatively high and stationary during the peak of the growing season (i.e., May–August, Figure 3b). In all treatments, NPP_W in both dominant and suppressed trees peaked in May or June and declined to a local

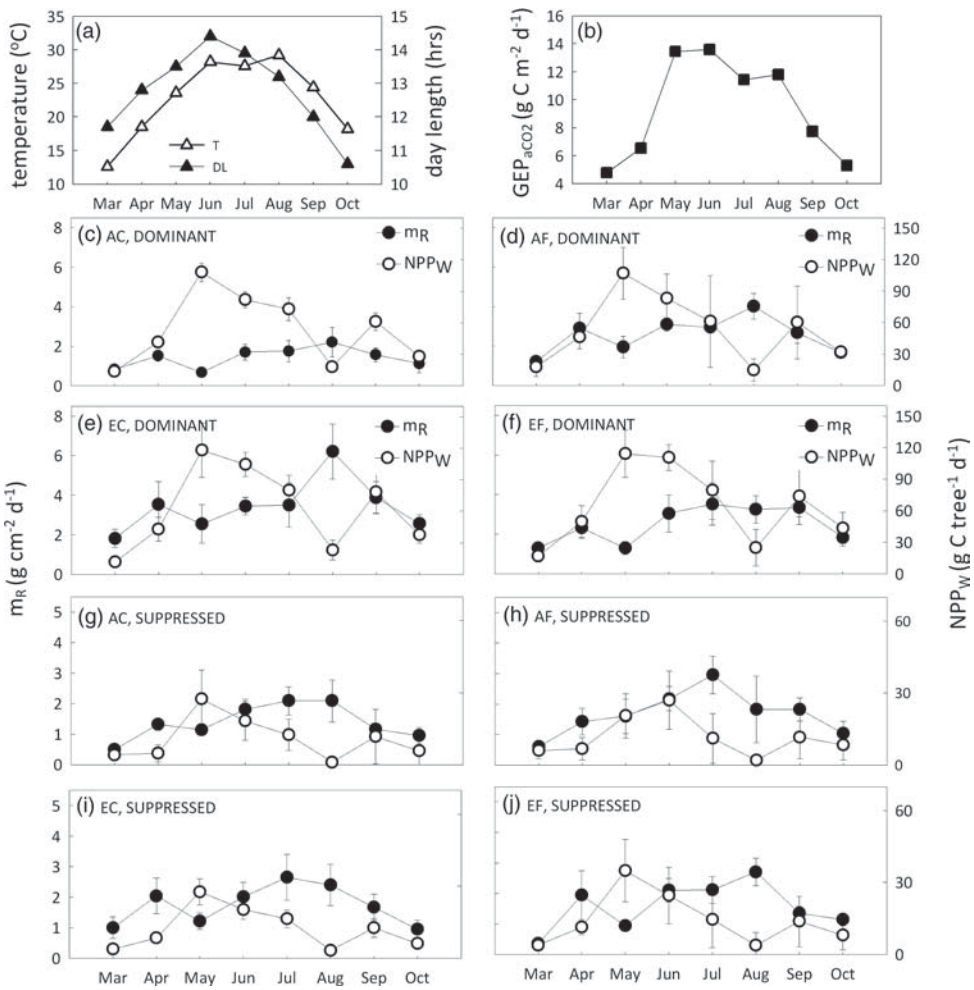

Figure 3. Temporal variation of key variables. Shown are mean monthly values of (a) temperature (*T*) and day length (DL), and (b) gross ecosystem production estimated over an ambient portion of the stand with the eddy-covariance technique (GEP_{aCO_2}). (c–f) Resin flow and NPP of woody biomass (m_R and NPP_W, respectively) for dominant trees from the four treatment classes: aCO_2 control (AC), aCO_2 fertilized (AF), eCO_2 control (EC) and eCO_2 fertilized (EF). (g–j) The same variables for suppressed trees. Symbols in (c–j) show the monthly averages from $n = 4$ subplots in each treatment class, with bars representing one standard error of the mean.

minimum in August (Figure 3c–j), concurrent with the development of a moderate soil moisture deficit which is typical in late summer. Conversely, the time series for m_R shows a local minimum in May and a local maximum later in the growing season (Figure 3c–j). Monthly variation in m_R was significant ($P < 0.01$, Table 1). The time series of m_R for all aCO_2 and eCO_2 individuals pooled is shown in Figure 4.

Temporal correlation among GEP_{aCO_2}, NPP_W and m_R

When GEP_{aCO_2} was relatively low (March–April, September–October), resin flow was directly related to both GEP_{aCO_2} and NPP_W ($P < 0.0001$, Figure 5a–d) in all treatments and size classes. In this presentation, m_R, GEP_{aCO_2} and NPP_W were normalized in reference to the study period maximum in each subplot to accommodate local differences in edaphic conditions and CO_2 concentration ($m_{R,N}$, $GEP_{aCO_2,N}$ and $NPP_{W,N}$, respectively). Conversely, when GEP_{aCO_2} was relatively high and stable (May–August), inverse relationships between $m_{R,N}$ and $NPP_{W,N}$ were observed for both size classes ($P < 0.0001$, Figure 5e and f).

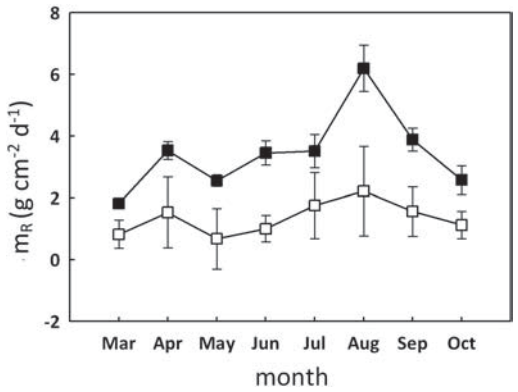

Figure 4. Effect of eCO_2 on resin flow time series. Monthly resin flow (m_R) in dominant, unfertilized trees growing in aCO_2 (AC, open symbols) and eCO_2 (EC, closed symbols), showing that the eCO_2 enhancement of m_R in these individuals persists throughout the growing season. Error bars show one standard error of the mean.

Table 1. Probability values for the impacts of atmospheric CO_2 concentration (C), fertilization (N) and sampling month (M) on resin flow (m_R) from a repeated-measures, split-plot ANOVA with CO_2 concentration as the main effect and fertilization treatment as the split effect. The ANOVA was run independently for dominant and suppressed trees, and significant effects are shown in bold type.

Effect	Df	m_R
Dominant ($n = 48$)		
C	**1**	**0.03**
N	1	0.78
C × N	1	0.13
M	**7**	**<0.01**
C × M	7	0.48
N × M	7	0.47
C × N × M	**7**	**0.01**
Suppressed ($n = 32$)		
C	1	0.97
N	1	0.60
C × N	1	0.63
M	**7**	**<0.01**
C × M	7	0.45
N × M	7	0.45
C × N × M	**7**	**0.02**

The similarity of the temporal response of $m_{R,N}$, $GEP_{aCO_2,N}$ and $NPP_{W,N}$ (Figure 5a–f) among treatments was evaluated by first formulating linear relationships between these two variables within each treatment using subplot-scale averages from all four subplots in each treatment. Then, for any two treatments, the residual error was estimated for a simplified model assuming the same slope and intercept for both treatments, and a full model assuming a separate slope and intercept for each treatment. The significance level of the reduction in error achieved by using the full versus simplified model was assessed via an *F*-test. In all cases, we found no differences in the relationships between $m_{R,N}$ and $GEP_{aCO_2,N}$ or $NPP_{W,N}$ among any of the treatments within each canopy class ($P = 0.46$–0.74).

Canopy size class effects

Throughout the study period, resin flow was significantly lower ($P = 0.01$) in suppressed compared with dominant trees ($\langle m_R \rangle \pm$ SD of 1.6 ± 0.7 and 2.5 ± 1.3 g cm^{-2} day^{-1}, respectively) when averaged across CO_2 and fertilization treatments. Net primary productivity of woody biomass was also signficantly lower ($P < 0.0001$) in suppressed compared with dominant trees ($\langle NPP_W \rangle \pm$ SD of 14 ± 4.5 and 60.2 ± 14.0 g C tree^{-2} day^{-1}, respectively). Gross ecosystem productivity was not measured separately for the different size classes. Temporal variation in m_R was significant in suppressed as well as dominant individuals (Table 1).

Elevated atmospheric CO_2 and N fertilization effects

The eCO_2 treatment significantly increased m_R among dominant individuals ($P = 0.03$, repeated-measures ANOVA, Table 1). This enhancement was entirely limited to trees growing in unfertilized subplots (Figure 6a), where eCO_2 increased m_R by 140% ($\langle m_R \rangle = 1.42 \pm 0.52$ and 3.44 ± 1.31 g cm^{-2} day^{-1} for AC and EC subplots, respectively). The eCO_2 enhancement persisted throughout the growing season (Figure 4). Atmospheric CO_2 concentration had no effect on m_R among fertilized individuals ($\langle m_R \rangle = 2.50 \pm 0.90$ and 2.50 ± 0.93 g cm^{-2} day^{-1} for AF and EF subplots, respectively, $P = 0.92$) and no effect among suppressed individuals regardless of N availability (Figure 6).

Spatial variation in mean m_R with N availability was evaluated for unfertilized and fertilized dominant and suppressed populations (Figure 6a and b). In each case, a linear model allowing unique slopes and intercepts for aCO_2 and eCO_2 populations

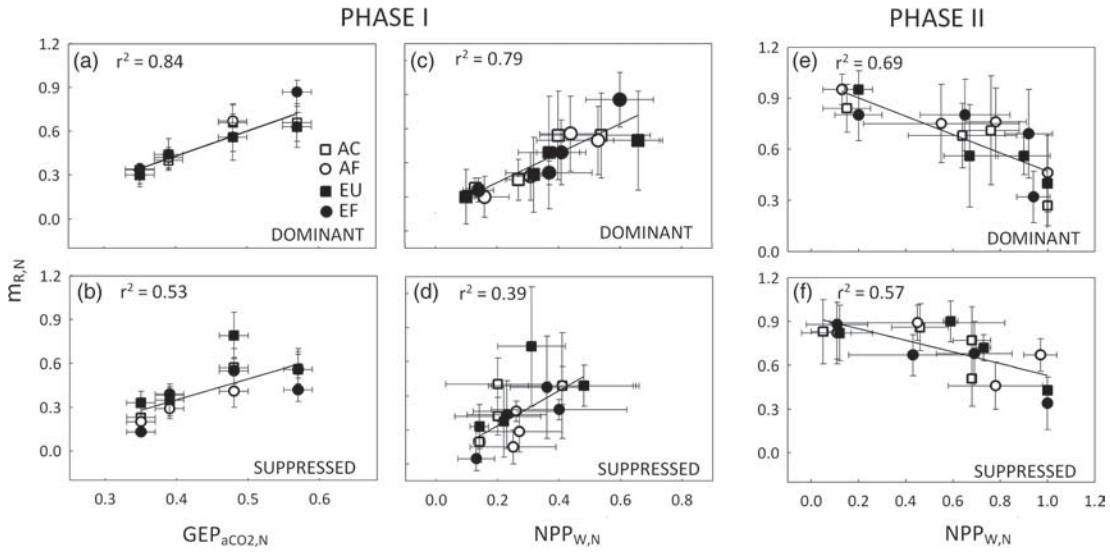

Figure 5. Relationships between normalized resin flow ($m_{R,N}$) and normalized eddy-covariance-based GEP ($GEP_{aCO_2,N}$) and normalized NPP of woody biomass ($NPP_{W,N}$). During Phase I (March–April and September–October; four left panels), $m_{R,N}$ is directly related to $GEP_{aCO_2,N}$ and to $NPP_{W,N}$ for dominant (upper panels) and suppressed (lower panels) individuals. In Phase II (May–August), $m_{R,N}$ was inversely related to $NPP_{W,N}$ (two right panels). The variables were normalized by the study period maximum in each subplot to accommodate local differences in edaphic conditions and CO_2 concentration. The variable GEP_{aCO_2} represents GEP of untreated conditions measured using the eddy-covariance technique over an ambient plot only. Symbols show the mean value in each treatment, and error bars show one standard error of the mean. Some data points are obscured by others, particularly in (a) and (b).

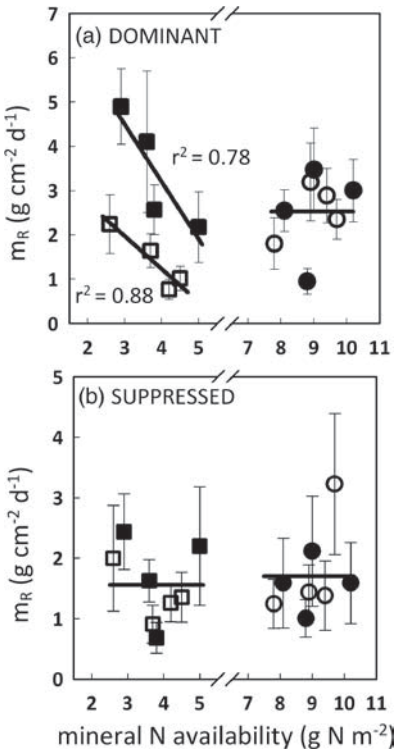

Figure 6. Spatial variation in subplot-scale m_R with mineral N availability is shown for unfertilized and fertilized dominant (a) and suppressed (b) populations. Among unfertilized dominants, a significant eCO_2 enhancement of m_R was observed ($P = 0.03$), and resin flow decreased significantly with native N availability ($P = 0.0002$). In all panels, error bars show one standard error of the mean. Symbols are as in Figure 4.

was compared with a simpler model assuming a single slope and intercept across CO_2 treatments. For unfertilized dominants, the full model offered a significant reduction in error ($P = 0.0002$, $r^2 = 0.92$) and suggested a decrease in m_R with N availability in both AC and EC populations (Figure 6a). In all other cases, the two models were statistically indistinguishable and none of the simple model slopes were statistically different from zero. While m_R decreased with native N availability among both AC and EC populations, the decrease was sharper for EC trees such that the eCO_2-induced enhancement decreased in unfertilized subplots as native N availability increased (from 2.6 to 4.5 g N m^{-2}, Figure 6a).

No significant variation in m_R with N availability or CO_2 treatment was observed for suppressed individuals (Table 1, Figure 6). Additionally, although m_R of all unfertilized dominant individuals pooled is significantly related to N availability (i.e., Figure 6a), the effect of fertilization on m_R is not significant (Table 1).

Both eCO_2 and fertilization increased NPP_W among our study trees, though the effects were not significant. However, the trends are consistent with other previous results from the FACE study showing significant enhancement to NPP_W under eCO_2 and with increasing N (McCarthy et al. 2010).

Discussion

Recently, large-scale bark beetle outbreaks have caused extensive tree mortality in several distinct infestations, including the ongoing mountain pine beetle (*Dendroctonus ponderosae*) outbreak in British Columbia, Canada that has

affected over 100,000 km^2 of lodgepole pine stands (Kurz et al. 2008), the recent outbreak of pinyon ips (*Ips confusus*) beetles in pinyon pine woodlands in southwestern North America (Raffa et al. 2008), and the outbreak of spruce beetles (*Dendroctonus rufipennis*) in white pine forests in Alaska in the 1990s (Berg et al. 2006). These outbreaks drew political and scientific attention to the effect of bark beetles on their host species (Negron et al. 2008) and the potential for increased severity of such damage in future climates (Gan 2004, Kurz et al. 2008). Bark beetle attacks are predicted to affect even larger areas in the future as warmer temperatures associated with climate change may be beneficial to beetle voltinism (Logan et al. 2003, Gan 2004, Berg et al. 2006, Kurz et al. 2008).

An important contributor to increased temperature is the rising concentration of atmospheric CO_2, and our study is the first to quantify the impact of eCO_2 on resin flow in mature pine trees. We show that eCO_2 signficantly enhances resin flow (by 140%) in dominant trees growing in low- to mid-range, but not high, fertility (Figure 6). We also show that while this enhancement persists throughout much of the year (Figure 4), the magnitude of resin flow varies significantly from month to month (Figure 3–5). In the following sections, we link these results to expectations from GDB theory and to previous observations of the effect of eCO_2 and fertilization on carbon assimilation and allocation in the study site. We also discuss the limitations of using GEP and NPP_W as proxies for A' and NPP.

Linking observed temporal trends and correlations to GDB expectations

As presented in Figure 1, the GDB hypothesis proposes that A', NPP and m_R will all be directly correlated provided A' is limited by some factor F (i.e., Phase I). When A' saturates with F, the former becomes stationary while growth continues to increase such that an inverse relationship between NPP and m_R is expected (Phase II). Often, F is interpreted to represent spatial gradients of nutrient availability, though it may represent any potentially limiting resource, including factors that vary in time (i.e., temperature, soil moisture content or even leaf area).

Measured GEP_{aCO_2}, which we use as a proxy for A', was relatively low at the beginning and the end of the growing season (i.e., March–April, September–October, Figure 2b), and with respect to temporal gradients of F, the study sites should be conceptually located in Phase I during these months (see Figure 1). As expected, direct correlations between GEP_{aCO_2}, m_R and NPP_W were observed during this time (Figure 5a–d). Conversely, when GEP_{aCO_2} was relatively high and stationary (May–August, Figure 3b), the study sites should be conceptually located in Phase II. And as expected, inverse relationships between NPP_W and m_R were observed during these months (Figure 5e and f). Thus, observed temporal variability in GEP_{aCO_2}, NPP_W and m_R largely conform to expectations from GDB theory.

The use of GPP and NPP_W as proxies for A' and NPP

Previously, direct estimates of A_{net} and the different components of NPP have been made for the AC and EC plots (Schäfer et al. 2003, McCarthy et al. 2010), permitting direct estimation of A' and NPP. However, monthly estimates of these variables are not available for our study period; therefore, we rely on GEP_{aCO_2} and NPP_W as proxies for A' and NPP. In this section, we discuss how temporal and spatial patterns of these proxies may differ from expected temporal and spatial trends in A' and NPP.

Gross ecosystem productivity is a gross assimilation flux, whereas A' is gross assimilation less maintenance respiration (i.e., $A' \sim GEP - R_M$). Therefore, treatment effects on the temporal evolution of R_M, which is primarily controlled by temperature and the amount of respiring biomass, may produce differences in the temporal pattern of A' across treatments. Temperature does not differ significantly among the treatment plots, and as we demonstrate in Figure 3c–j, patterns of NPP_W (and hence biomass accumulation) are also similar across treatments. We note that foliage biomass, the plant component contributing most to R_M, was shown to have similar dynamics among aCO_2 and eCO_2 treatments (Schäfer et al. 2003, McCarthy et al. 2007). The effect of fertilization on the seasonality of leaf area production is not yet known for the study site, though previous work has shown that fertilization does not affect the seasonal pattern of shoot and foliage development in loblolly pine (Zhang et al. 1997). Thus, we have no reason to expect that the treatments promoted significant differences in the dynamics of R_M.

Treatment effects on leaf phenology may also influence the temporal patterns of GEP, which we have assumed to be similar across treatments in this analysis. Again, we do not expect large differences in the seasonality of leaf area production across sites. Furthermore, as most leaf area production occurs during May–July (i.e., Phase II), it is unlikely that plot-specific differences in leaf area expansion would affect the delineation between Phase I (March–April, September–October) and Phase II (May–August). Similarly, it is also unlikely that site-specific differences in leaf area expansion would strongly affect Phase I temporal relationships between $m_{R,N}$ and $GEP_{aCO_2,N}$ shown in Figure 5a and b. Variations in A' are not explicitly considered in the formulation of the relationships between $m_{R,N}$ and $NPP_{W,N}$ (Figure 5c–f), and our interpretation of the results relies on the practical assumption that A' is high and stationary during Phase II months. Clearly, uncertainty attributed to temporal variation in A' during Phase II months (i.e., Figure 3b), as well as site-specific differences in A', may contribute to some of the unexplained variation between $m_{R,N}$ and $NPP_{W,N}$.

Because $NPP = NPP_W + NPP_{foliage} + NPP_{fine\text{-}root}$, the dynamics of NPP_W might differ from that of NPP if leaf biomass production ($NPP_{foliage}$) and fine root production ($NPP_{fine\text{-}root}$) are a large proportion of total NPP and follow a different seasonal pattern from NPP_W. Developing an estimate of NPP for this analysis is difficult for a number of reasons. First, some of the relevant variables (including leaf and fine root expansion) are not available for 2009. Second, NPP must be specified at the same scale as resin flow (i.e., the tree scale) and independently for dominant and suppressed populations, which requires assumptions regarding the extent to which patterns in leaf and woody biomass production differ with tree size. Despite these challenges, we produced estimates of monthly NPP for each treatment class during our study period and found strong correlation between NPP and NPP_W within dominant ($r = 0.96$) and suppressed ($r = 0.94$) populations. Nevertheless, we elected to use NPP_W instead of NPP in this investigation because this estimate of growth contains much less uncertainty both in time and among populations than NPP. Furthermore, it can be argued that the most direct competition with resin production is the local wood production sink for carbohydrates. Resin synthesis occurs in the stem, and the availability of carbohydrates for resin production and stem growth is controlled by both the size of the source and transport processes moving carbohydrates from leaves to the stem.

Treatment effects on the relative magnitude of assimilation and growth are not explicitly considered in this analysis, though they are important for the interpretation of the results, and in particular the discussion presented in the next section. Increases in GEP related to eCO_2 or fertilization should also enhance A', provided that these treatments do not produce an enhancement to R_M of similar magnitude. This is most certainly the case for eCO_2, which enhances net canopy assimilation by 400–1000 g C m^{-2} $year^{-1}$ (Schäfer et al. 2003) through increases in both leaf-level assimilation capacity (Maier et al. 2008) and total leaf area (McCarthy et al. 2007), while enhancing R_M by <100 g C m^{-2} $year^{-1}$ (Schäfer et al. 2003). Enhancements to NPP_W in EC as compared with AC subplots should also be accompanied by similar enhancement to NPP, as previous work has shown that eCO_2 does not affect the partitioning of assimilated carbon among plant biomass pools (McCarthy et al. 2010). On the other hand, the ratio of NPP_W/NPP may not be constant between fertilized and control sectors as fertilization affects the ratio of belowground to aboveground carbon allocation (Palmroth et al. 2006). Such a shift in partitioning may explain the increase in resin flow observed in AF as compared with AC plots as discussed in the following section.

Linking observed spatial variability in m_R to GDB predictions

In forests of dense, light-limited canopies, increased nutrient availability typically enhances growth more than photosynthesis (e.g., $\partial(A' - NPP)/\partial F < 0$, where F is nutrient availability) because carbon investment in leaf area results in diminishing returns of absorbed light (Palmroth et al. 2006). Thus, when F represents spatial gradients of nutrient availability, the plots of the study site fit conceptually in Phase II of Figure 1, and GDB theory would predict a decrease in m_R with increasing soil fertility. Indeed, resin flow of dominant trees grown in both eCO_2 and aCO_2 subplots was inversely related to native N availability (Figure 6a).

The observed effects of eCO_2 on m_R also agree with predictions from the GDB hypothesis. Namely, eCO_2 increased resin flow in plots of low- to mid-range, but not high, soil fertility (Figure 6). Previous work at the Duke FACE experiment has shown that eCO_2 stimulates photosynthesis by ~40% in unfertilized plots (Schäfer et al. 2003, Maier et al. 2008) with no further enhancement expected with N addition (Palmroth et al. 2006, Maier et al. 2008), yet enhances NPP by only 18% in nutrient-poor plots compared with 30% in richer plots (McCarthy et al. 2010). Thus, the observation that dominant trees in the EC subplots have greater m_R is consistent with a larger $A' - NPP$ balance in these trees relative to AC populations.

We note that among eCO_2 trees, N amendment did not increase m_R relative to trees in the plots with the highest native N availability ($P = 0.58$ of EF versus highest EC). Yet, resin flow increased in dominant AF versus AC trees in high native N subplots (Figure 6a, $P = 0.007$)—an observation that does not agree with the GDB predictions. There are two possible explanations for the observed discrepancy. The first is that fertilization increased both assimilation and growth in AF subplots, but with a relatively larger increase in assimilation. Earlier work has shown that fertilization tends to increase leaf area production in aCO_2 plots by ~20–25%, though the effect is not significant (McCarthy et al. 2007). Fertilization has also been shown to significantly increase leaf-level assimilation capacity (i.e., A_{net}) in aCO_2 plots, with an 18% increase for current-year foliage (Figure 2; see also Maier et al. 2008). Consequently, increases in leaf area and leaf-level assimilation capacity may have resulted in $\partial(A' - NPP)/\partial F > 0$ by increasing $\partial A'/\partial F$ with increasing N. In eCO_2 subplots, canopy leaf area was already 25% higher than aCO_2 subplots and substantial gains in leaf area with fertilization were not possible. Thus, in eCO_2 subplots, little additional gain in $\partial A'/\partial F$ is expected with increasing N.

The second explanation is that under fertilization, partitioning of carbon was redirected from belowground processes to aboveground processes (Palmroth et al. 2006), and could thus support increases of both growth and m_R in apparent contradiction of the GDB scheme. However, if the latter is the dominant reason, the effect should have been noticeable under eCO_2 as well, and thus the behavior seems more consistent with our first explanation.

Table 2. Synthesis of published studies that observed the impact of fertilization on resin flow.

Species	Location	Age	Other treatments	Fertilization effect	Reference
Pinus sylvestris	Harjavalta, Finland	60–90	…	No effect	Kyto et al. (1999)
Pinus sylvestris	Harjavalta, Finland	60–90	Defoliated	No effect	Kyto et al. (1999)
Pinus taeda	Louisiana, USA	25	…	No effect	Lombardero et al. (2000)
Pinus taeda	Louisiana, USA	25	Thinned	No effect	Lombardero et al. (2000)
Pinus taeda	Louisiana, USA	15	…	No effect	Ruel et al. (1998)
Pinus taeda	Louisiana, USA	13	Thinned	m_R decreased	Wilkens et al. (1998)
Pinus taeda	Louisiana, USA	13	…	No effect	Wilkens et al. (1998)
Pinus taeda	North Carolina, USA	16	…	No effect	Klepzig et al. (2005)
Pinus taeda	North Carolina, USA	16	Irrigated	No effect	Klepzig et al. (2005)
Pinus taeda	North Carolina, USA	6	…	m_R increased	Knebel et al. (2008)
Pinus taeda	North Carolina, USA	12	…	m_R increased	Knebel et al. (2008)
Pinus taeda	North Carolina, USA	11	…	m_R decreased	Warren et al. (1999)
Pinus taeda	Virginia, USA	24	…	No effect	Matson et al. (1987)
Pinus taeda	Virginia, USA	24	Thinned	No effect	Matson et al. (1987)

Resin flow in suppressed individuals

In the sub-canopy, light limitations significantly reduce GPP in suppressed individuals (Schäfer et al. 2003) such that light may be the primary limiting resource to assimilation in these individuals. In this study, NPP_W was also lower for suppressed trees. However, during the beginning and end of the growing season (i.e., March–April, September–October), m_R scaled with GEP_{aCO_2} and NPP_W among suppressed individuals (Figure 5b and d), suggesting that $\partial(A' - NPP)/\partial F$ is nonetheless positive. During the peak of the growing season (May–August), when leaf area (and light penetration in the canopy) is relatively stationary, inverse relationships between GEP_{aCO_2} and m_R were observed (Figure 5f). These results follow expectations from GDB theory if GEP_{aCO_2} was also stationary among suppressed individuals during this portion of the study period. In space, the fertilization and eCO_2 treatments had no effect on m_R in suppressed individuals (Figure 6b), which is consistent with GDB predictions if light is indeed more limiting to their photosynthesis than N availability or atmospheric CO_2 concentration.

Implications

The Duke FACE experiment permitted us to quantify for the first time the effect of elevated atmospheric CO_2 on resin flow of mature, field-grown pine trees in the context of carbon source–sink interactions, utilizing variation in the balance of $A' - NPP$ induced spatially by both N availability and tree position in the canopy, and temporally by seasonal dynamics. Following predictions based on the GDB scheme, eCO_2 enhanced resin flow in dominant trees. The absolute enhancement was most clear during periods when growth was seasonally low (Figures 3d–j and 4) or limited by N availability (Figure 6a). Prior studies have shown that tree mortality during bark beetle attacks follows threshold dynamics driven by plant defense properties and the number of attacking beetles (Waring and Pitman 1985, Coops et al. 2009). Thus, the observed eCO_2-induced enhancement of resin should be considered when making predictions about the frequency and severity of bark beetle attacks in future climates, at least in forests with low- to mid-range fertility, which currently represent the majority of southern pine forests (Fox et al. 2007). Indeed, previous studies have shown that even more modest increases in resin flow (i.e., enhancements ≤ 100%) significantly increase the survival probability of pine trees experiencing bark beetle attack (Reeve et al. 1995, Strom et al. 2002).

Under current atmospheric CO_2 concentrations, fertilization may increase resin flow (as observed in the ambient plots in this study) or may have no effect on resin flow (as demonstrated in the majority of studies investigating the response of m_R to fertilization) (see Table 2). However, under future conditions when protection from increased attacks is needed, fertilization may reduce pine resistance to beetles. Moreover, any changes in weather patterns that enhance NPP (e.g., longer growing season) or that limit A' (e.g., severe drought) will likely do so at the expense of resin production. In unmanaged, dense stands, which cover vast areas of temperate and boreal forests, many individuals are effectively suppressed with a small $A' - NPP$ balance. This study suggests that resistance to bark beetle attack in suppressed trees will not increase with CO_2, regardless of soil fertility.

Acknowledgments

We acknowledge Eric Ward and Sari Palmroth for feedback on the analysis, and Jeff Pippen, Andrea Casanova and Javier Luscarain for data collection assistance. We also acknowledge three anonymous reviewers for insightful comments on the manuscript. We thank Fred Hain and John Strider for methodological and material assistance.

Funding

This research was sponsored by the Office of Science (BER), US Department of Energy (FG02-95SER62083), and by the NSF Graduate Research Fellowship Program (DGE1106401) and the James B. Duke Fellowship Program.

References

Berg, E.E., J.D. Henry, C.L. Fastie, A.D. De Volder and S.M. Matsuoka. 2006. Spruce beetle outbreaks on the Kenai Peninsula, Alaska, and Kluane National Park and Reserve, Yukon Territory: relationship to summer temperatures and regional differences in disturbance regimes. For. Ecol. Manag. 227:219–232.

Coops, N.C., R.H. Waring, M.A. Wulder and J.C. White. 2009. Prediction and assessment of bark beetle-induced mortality of lodgepole pine using estimates of stand vigor derived from remotely sensed data. Remote Sens. Environ. 113:1058–1066.

Ellsworth, D.S. 1999. CO_2 enrichment in a maturing pine forest: are CO_2 exchange and water status in the canopy affected? Plant Cell Environ. 22:461–472.

Finzi, A.C., D.J.P. Moore, E.H. DeLucia, *et al.* 2006. Progressive N limitation of ecosystem processes under elevated CO_2 in a warm temperature forest. Ecology 87:15–25.

Fox, T.R., E.J. Jokela and H.L. Allen. 2007. The development of pine plantation silviculture in the southern United States. J. For. 105:337–347.

Gan, J.B. 2004. Risk and damage of southern pine beetle outbreaks under global climate change. For. Ecol. Manag. 191:61–71.

Goulden, M.L., B.C. Daube, S.-M. Fan, D.J. Sutton, A. Bazzaz, J.W. Munger and S.C. Wofsy. 1997. Physiological responses of a black spruce forest to weather. J. Geophys. Res. Atmos. 102:28987–28996.

Hendrey, G.R., D.S. Ellsworth, K.F. Lewin and J. Nagy. 1999. A free-air enrichment system for exposing tall forest vegetation to elevated atmospheric CO_2. Glob. Change Biol. 5:293–309.

Herms, D.A. and W.J. Mattson. 1992. The dilemma of plants—to grow or defend. Q. Rev. Biol. 67:283–335.

Hofmockel, K.S. and W.H. Schlesinger. 2007. Carbon dioxide effects on heterotrophic dinitrogen fixation in a temperate pine forest. Soil. Sci. Soc. Am. J. 71:140–144.

Johnsen, K., B. Teskey, L. Samuelson, J. Butnor, D. Sampson, F. Sanchez, C. Maier and S. McKeand. 2004. Carbon sequestration in loblolly pine plantations: methods, limitations, and research needs for estimating storage pools. *In* Southern Forest Science: Past, Present, and Future. GTR-SRS-75. Eds. M.H. Rauscher and K. Johnsen. USDA Forest Service, Southern Research Station, Asheville.

Klepzig, K.D., D.J. Robison, G. Fowler, P.R. Minchin, F.P. Hain and H.L. Allen. 2005. Effects of mass inoculation on induced oleoresin response in intensively managed loblolly pine. Tree Physiol. 25:681–688.

Knebel, L., D.J. Robison, T.R. Wentworth and K.D. Klepzig. 2008. Resin flow responses to fertilization, wounding and fungal inoculation in loblolly pine (*Pinus taeda*) in North Carolina. Tree Physiol. 28:847–853.

Kurz, W.A., C.C. Dymond, G. Stinson, G.J. Rampley, E.T. Neilson, A.L. Carroll, T. Ebata and L. Safranyik. 2008. Mountain pine beetle and forest carbon feedback to climate change. Nature 452:987–990.

Kyto, M., P. Niemela, E. Annila and M. Varama. 1999. Effects of forest fertilization on the radial growth and resin exudation of insect-defoliated Scots pines. J. Appl. Ecol. 36:763–769.

Lapasha, C.A. and E.A. Wheeler. 1990. Resin canals in *Pinus taeda*: longitudinal canal lengths and interconnections between longitudinal and radial can. IAWA Bull. 11:227–238.

Logan, J.A., J. Regniere and J.A. Powell. 2003. Assessing the impacts of global warming on forest pest dynamics. Front. Ecol. Environ. 1:130–137.

Lombardero, M.J., M.P. Ayres, P.L. Lorio and J.J. Ruel. 2000. Environmental effects on constitutive and inducible resin defences of *Pinus taeda*. Ecol. Lett. 3:329–339.

Lorio, P.L. 1986. Growth-differentiation balance—a basis for understanding southern pine-beetle tree interactions. For. Ecol. Manag. 14:259–273.

Lorio, P.L., F.M. Stephen and T.D. Paine. 1995. Environment and ontogeny modify loblolly-pine response to induced acute water deficits and bark beetle attack. For. Ecol. Manag. 73:97–110.

Maier, C.A., S. Palmroth and E. Ward. 2008. Short-term effects of fertilization on photosynthesis and leaf morphology of field-grown loblolly pine following long-term exposure to elevated CO_2 concentration. Tree Physiol. 28:597–606.

Matson, P.A., F.P. Hain and W. Mawby. 1987. Indices of tree susceptibility to bark beetles vary with silvicultural treatment in a loblolly pine plantation. For. Ecol. Manag. 22:107–188.

McCarthy, H.R., R. Oren, A.C. Finzi, D.S. Ellsworth, H.S. Kim, K.H. Johnsen and B. Millar. 2007. Temporal dynamics and spatial variability in the enhancement of canopy leaf area under elevated atmospheric CO_2. Glob. Change Biol. 13:2479–2497.

McCarthy, H.R., R. Oren, K.H. Johnsen, A. Gallet-Budynek, S.G. Pritchard, C.W. Cook, S.L. LaDeau, R.B. Jackson and A.C. Finzi. 2010. Re-assessment of plant carbon dynamics at the Duke free-air CO_2 enrichment site: interactions of atmospheric CO_2 with nitrogen and water availability over stand development. New Phytol. 185:514–528.

McDowell, N.G., H.D. Adams, J.D. Bailey and T.E. Kolb. 2007. The role of stand density on growth efficiency, leaf area index, and resin flow in southwestern ponderosa pine forests. Can. J. For. Res. 37:343–355.

Negron, J.F., B.J. Bentz, C.J. Fettig, *et al.* 2008. US Forest Service bark beetle research in the western United States: looking toward the future. J. For. 106:325–331.

Oren, R., D.S. Ellsworth, K.H. Johnsen, *et al.* 2001. Soil fertility limits carbon sequestration by forest ecosystems in a CO_2-enriched atmosphere. Nature 411:469–472.

Palmroth, S., C.A. Maier, H.R. McCarthy, A.C. Oishi, H.S. Kim, K.H. Johnsen, G.G. Katul and R. Oren. 2005. Contrasting responses to drought of forest floor CO_2 efflux in a loblolly pine plantation and a nearby oak-hickory forest. Glob. Change Biol. 11:421–434.

Palmroth, S., R. Oren, H.R. McCarthy, K.H. Johnsen, A.C. Finzi, J.R. Butnor, M.G. Ryan and W.H. Schlesinger. 2006. Aboveground sink strength in forests controls the allocation of carbon below ground and its [CO_2] - induced enhancement. Proc. Natl Acad. Sci. USA 103:19362–19367.

Papale, D., M. Reichstein, M. Aubinet, *et al.* 2006. Towards a standardized processing of net ecosystem exchange measured with eddy covariance technique: algorithms and uncertainty estimation. Biogeosciences 3:571–583.

Phillips, R.L., S.C. Whalen and W.H. Schlesinger. 2001. Influence of atmospheric CO_2 enrichment on nitrous oxide flux in a temperate forest. Glob. Biogeochem. Cy. 15:741–752.

Price, T., C. Doggett, J. Pye and B. Smith. 1998. A history of southern pine beetle outbreaks in the southeastern United States. Georgia Forestry Commission, Atlanta, GA.

Raffa, K.F., B.H. Aukema, B.J. Bentz, A.L. Carroll, J.A. Hicke, M.G. Turner and W.H. Romme. 2008. Cross-scale drivers of natural disturbances prone to anthropogenic amplification: the dynamics of bark beetle eruptions. Bioscience 58:501–517.

Reeve, J.D., M.P. Ayres, P.L. Lorio, Jr, N. Cappuccino and P.W. Price. 1995. Host suitability, predation, and bark beetle population dynamics. *In* Population Dynamics: New Approaches and Synthesis. Eds. N.

Cappuccino and P.W. Price. Academic Press, San Diego, pp 339–357.

Reichstein, M., E. Falge, D. Baldocchi, *et al.* 2005. On the separation of net ecosystem exchange into assimilation and ecosystem respiration: review and improved algorithm. Glob. Change Biol. 11:1424–1439.

Ruel, J.J., M.P. Ayres and P.L. Lorio. 1998. Loblolly pine responds to mechanical wounding with increased resin flow. Can. J. For. Res. 28:596–602.

Schäfer, K.V.R., R. Oren, D.S. Ellsworth, C.T. Lai, J.D. Herrick, A.C. Finzi, D.D. Richter and G.G. Katul. 2003. Exposure to an enriched CO_2 atmosphere alters carbon assimilation and allocation in a pine forest ecosystem. Glob. Change Biol. 9:1378–1400.

Sparks, J.P., J. Walker, A. Turnipseed and A. Guenther. 2008. Dry nitrogen deposition estimates over a forest experiencing free air CO_2 enrichment. Glob. Change Biol. 14:768–781.

Stamp, N. 2004. Can the growth-differentiation balance hypothesis be tested rigorously? Oikos 107:439–448.

Stoy, P.C., G.G. Katul, M.B.S. Siqueira, J.Y. Juang, K.A. Novick, J.M. Uebelherr and R. Oren. 2006. An evaluation of models for partitioning eddy covariance-measured net ecosystem exchange into photosynthesis and respiration. Agric. For. Meteorol. 141:2–18.

Strom, B.L., R.A. Goyer, L.L. Ingram, Jr, G.D.L. Boyd and L.H. Lott. 2002. Oleoresin characteristics of progeny of loblolly pines that escaped attack by the southern pine beetle. For. Ecol. Manag. 157:169–178.

Wallin, K.F., T.E. Kolb, K.R. Skov, and M. Wagner. 2008. Forest management treatments, tree resistance, and bark beetle resource utilization in ponderosa pine forests of northern Arizona. For. Ecol. Manag. 255:3263–3269.

Waring, R.H. and G.B. Pitman. 1985. Modifying lodgepole pine stands to change susceptibility to mountain pine-beetle attack. Ecology 66:889–897.

Warren, J.M., H.L. Allen and F.L. Booker. 1999. Mineral nutrition, resin flow and phloem phytochemistry in loblolly pine. Tree Physiol. 19:655–663.

Wilkens, R.T., M.P. Ayres, P.L. Lorio, Jr and J.D. Hodges. 1998. Environmental effects on pine tree carbon budgets and resistance to bark beetles. *In* The Productivity and Sustainability of Southern Forest Ecosystems in a Changing Environment. Eds. R.A. Mickler and S. Fox. Springer, New York, pp 591–616.

Zhang, S.S., H.L. Allen and P.M. Dougherty. 1997. Shoot and foliage growth phenology of loblolly pine trees as affected by nitrogen fertilization. Can. J. For. Res. 27:1420–1426.